Article

Not peer-reviewed version

Maresin-like 1 Ameliorates Neuropathology of Alzheimer's Disease in Brains of a Transgenic Mouse Model

Pallavi Shrivastava , Yan Lu , Shanchun Su , Yuichi Kobayashi , Yuhai Zhao , Nathan Lien , Abdul-Razak Masoud , Walter J Lukiw , Song Hong *

Posted Date: 27 September 2024

doi: 10.20944/preprints202407.0723.v2

Keywords: Maresin-like; Alzheimer's Disease; neuroinflammation; neuropathogenesis; amyloid-β (Aβ); cholinergic neuron; cleaved-caspase-3; M1 or M2 microglia; N1 or N2 neutrophil

Article

Maresin-like 1 Ameliorates Neuropathology of Alzheimer's Disease in Brains of a Transgenic Mouse Model

Pallavi Shrivastava [1], Yan Lu [1], Shanchun Su [1], Yuichi Kobayashi [2,3], Yuhai, Zhao [1], Nathan Lien [1], Abdul-Razak Masoud [1], Walter J Lukiw [1,†] and Song Hong [1,*,†]

[1] Neuroscience Center of Excellence, School of Medicine, Louisiana State University Health, New Orleans, 2020 Gravier St., New Orleans, LA 70112, USA
[2] Department of Bioengineering, Tokyo Institute of Technology, Box B-52, Nagatsuta-cho 4259, Midori-ku, Yokohama 226-8501, Japan
[3] Organization for the Strategic Coordination of Research and Intellectual Properties, Meiji University, 1-1-1 Higashimita, Tama-ku, Kawasaki 214-8571, Japan
* Correspondence: shong@lsuhsc.edu
† Department of Ophthalmology, School of Medicine, Louisiana State University Health, New Orleans, 2020 Gravier St., New Orleans, LA 70112, USA.

Abstract: 1) Background: Impeded resolution of inflammation contributes substantially to the pathogenesis of Alzheimer's disease (AD); consequently, resolving inflammation is pivotal to the amelioration of AD pathology. This can potentially be achieved by the treatment with specialized pro-resolving lipid mediators (SPMs), which should resolve neuroinflammation in brains. 2) Methods: Here, we report the effects of long-term treatment with a SPM, maresin like 1 (MarL1), on AD pathogenesis in a transgenic 5xFAD mouse model. 3) Results: MarL1 treatment reduced Aβ overload, curbed the loss of neurons in brains especially cholinergic neurons associated with cleaved-caspase-3-associated apoptotic degeneration, reduced microgliosis and the pro-inflammatory M1 polarization of microglia, curbed the AD-associated decline in anti-inflammatory Iba1^{+}Arg-1^{+}-M2 microglia, inhibited phenotypic switching to pro-inflammatory N1 neutrophils, promoted the blood–brain-barrier-associated tight-junction protein claudin-5 and decreased neutrophil leakage in 5xFAD brains, and induced the switch of neutrophils toward the inflammation-resolving N2 phenotype. 4) Conclusion: Long-term administration of MarL1 mitigates AD-related neuropathogenesis in brains by curbing neuroinflammation and neurodegeneration. These findings provided the preclinical leads and mechanistic insights for the development of MarL1 into an effective modality to ameliorate AD pathogenesis.

Keywords: Maresin-like; Alzheimer's Disease; neuroinflammation; neuropathogenesis; amyloid-β (Aβ); cholinergic neuron; cleaved-caspase-3; M1 or M2 microglia; N1 or N2 neutrophil

1. Introduction

Alzheimer's disease (AD) affects more than 6.5 million people over the age of 65 years in the United States alone [1] and 50 million people worldwide [2]. Typical neuropathological characteristics of AD include the accumulation of amyloid-β (Aβ) peptide in brain parenchyma and perivascular regions as senile plaques, and an accompanying synaptic and neuronal loss mainly in the hippocampal and cortical regions of the brain [3].

AD progression is greatly affected by the neuroinflammatory reactions [4]. Abnormal aggregation of Aβ is identified as one of the primary factors [5]. Recognition of the significance of neuroinflammation in AD has brought more attention to specialized pro-resolving mediators (SPMs). These types of mediators effectively promote the resolution of inflammation [6]. One class of these

 doi:10.20944/preprints202407.0723.v

compounds are maresins that were discovered by Serhan et al. [7,8]. Maresins and the related maresin -like (MarL) mediators [9] are derived from essential ω-3 docosahexaenoic acid (DHA) by the action of endogenous enzymatic systems [12- or 15-lipoxgenase (LO) for maresins; and 12/15-LO combined with a cytochrome P450 CYP4F3 for MarL]. Maresin-1 (7*R*,14*S*-dihydroxy-4*Z*,8*E*,10*E*,12*Z*,16*Z*,19*Z*-DHA) reduces neuroinflammation, mitochondrial damage, and neuronal death, while enhancing neural functional recovery, phagocytosis of Aβ, and the switch in macrophage phenotype to the anti-inflammatory M2 type [10,11]. Maresin-1 improves the pathological condition of experimental autoimmune encephalomyelitis [12]. In Aβ42 treated C57BL/6 mice, cognitive decline and neuroinflammation is alleviated by maresin-1 treatment [13]. Similarly, in another AD mouse model ($App^{NL\text{-}G\text{-}F/NL\text{-}G\text{-}F}$), microglial activation has been significantly reduced by the intranasal instillation of a group of SPMs including maresin- 1 [14].

In contrast, the maresin-like compound MarL1 (14*S*,22-dihydroxy-docosa-4*Z*,7*Z*,10*Z*,12*E*,16*Z*,19*Z*-hexaenoic acid) promotes the release of the regenerative angiogenic growth factor HGF and reduces the expression of inflammatory cytokine TNF*α* in macrophages in vitro [9]. MarL1 recovers macrophage the functions in the elevation of migration of epithelial cells and fibroblasts in scratch-wounded monolayer cultures, as well as stem cell transmigration [9]. Despite the growing evidence for pro-resolving and neuroprotective effects of maresin-1 and MarLs, the underlying mechanisms require further investigation for their therapeutic development. In the present study, we have hypothesized that long-term administration of MarL1 administration could mitigate AD-related brain neuropathogenesis by curbing neuroinflammation and neurodegeneration.

The 5x familial Alzheimer's Disease (5xFAD) transgenic mouse overexpress humanized sequences of five AD-linked mutations including the Swedish (K670N/M671L), Florida (I716V), and London (V717I) mutations in APP and the M146L and L286V mutations in PSEN1 under the regulation of the neuron-specific thy1 promoter [15]. The most prominent feature of 5xFAD mice is that they present AD amyloid pathology and neuron loss at young age [15,16].

Neuroinflammation starts as early as 2–3 months of age in 5xFAD mice [15]. Pro-inflammatory M1-phenotype microglia are major contributors and indicate the occurrence of the neuroinflammation [17–19]. As resident immune cells of the central nervous system, resting microglia continuously survey the microenvironment of the brain [20]. Under adversary condition, microglia become activated and transfer to either M1 or M2 phenotype [21]. M1 type microglia adopt an amoeboid shape [22], and are highly phagocytic and expressing CD68 in high level [23]. In contrast, alternative M2 microglia play an important role in immuno-resolution and repair processes during an injury, exhibiting neuroprotective effects [24,25]. The switching between M1 and M2 phenotypes relies on the severity and progression of the disease [26,27].

Neutrophils generally are scarce in healthy brain due to the brain-blood barrier (BBB) [28]. Under neuroinflammatory conditions, neutrophils are observed to promote the BBB damage and transmigrate into brain parenchyma [29–31]. There have been reports on the increase in the neutrophil population in different models of AD [32,33]. Neutrophils penetrate the brain parenchyma by breaching BBB and move toward amyloid plaques in the 5xFAD mouse model [34]. Analogous to the conventional categorization of macrophages or microglia into two major types, M1 and M2 phenotypes, neutrophils have been categorized into pro-inflammatory N1 [35] and anti-inflammatory N2 subpopulations [36]. Their transcriptomic profiles are distinctive [35]. N1 and N2 neutrophils function differently in neuroinflammation [37]. N1 neutrophils exhibit a remarkably increased production of reactive oxygen species (ROS) as well as nitric oxide (NO). By contrast, N2 neutrophils demonstrate increased expression of Arginase 1 (Arg1) [35,37]. We have determined the possible occurrence of N1 and N2 neutrophils in brains of 5xFAD mice with and without treatment as well as of wildtype control mice in this study.

 doi:10.20944/preprints202407.0723.v

2. Materials and Methods

2.1. Animals

The Louisiana State University Health Science Center (LSUHSC) IACUC committee approved all the animal procedures, which are consistent with American Veterinary Medical Association guidelines. Mice were maintained at LSUHSC at a controlled temperature of 25 ± 2°C and 50%–65% humidity with a fixed 12:12 h light-dark cycle. We used a widely used model of AD—5xFAD transgenic mice (Jackson Laboratory, Bar Harbor, ME, USA) with a C57BL/6J genetic background (MMRRC Strain #034840-JAX)—and compared them with wildtype (WT) control mice (C57BL/6J) [38].

2.2. Intranasal Treatment with Maresin-Like 1

Male mice at the age of 1.5 months were randomly selected and equally divided into the following three groups: 1) WT (C57BL/6J mice), 2) 5xFAD mice treated with vehicle, and 3) 5xFAD mice treated with MarL1 plus vehicle. The MarL1 or vehicle was administered by the intranasal route 3 times per week to each mouse from 1.5 months to 9 months of age. Briefly, each mouse was temporarily immobilized for about 60 seconds by a slight anesthetization using isoflurane inhalation. While the mouse was immobilized, it was held in the supine position and its nostrils were then instilled with 3 µL/nostril of MarL1 (100 ng per mouse for each administration) dissolved in the vehicle (0.05% dimethyl sulfoxide [DMSO] in sterile 0.9% saline) or with 3 µL the vehicle alone. The mouse was held at the same position for 20 more seconds to ensure liquid intranasal intake [14,39–41]. The mice were sacrificed at the age of 12.5 months.

2.3. Harvesting of Murine Brains for Immunohistology

The mice were anesthetized with 5% isoflurane and subsequently perfused transcardially with 4% paraformaldehyde (PFA). The change in liver color from deep red to a lighter shade was used to indicate adequate perfusion. The mice were then decapitated and the brains were quickly removed and immersed in 4% PFA overnight at 4°C. After 24 hours, the brains were placed in a 15% sucrose solution for 12 hours, followed by a 30% sucrose solution until they sank. The brain tissue was then embedded in optimal cutting temperature compound (OCT) and cryo-molds for cryo-sectioning. Coronal section of brains was serially cut from rostral to caudal at 20 µm thickness on a HM550 cryostat (Microm-HM 550, Thermo Fisher Scientific). These sections were then mounted on Superfrost Plus glass slides (VWR, Radnor, PA, USA), and sections from the cortex and hippocampus regions were selected for immunofluorescence.

2.4. Immunofluorescence Staining

The mounted brain sections (containing cortex and hippocampus) were washed twice in phosphate-buffered saline (PBS), followed by two washes in PBS-T (PBS containing 0.05% Triton-X). The sections were then incubated in blocking buffer (1% BSA+0.5% Trition-X+0.02% Tween-20 in 1X PBS) at room temperature for 60 min. The sections were then treated with the following antibodies: NeuN (1:500, rabbit, cell signaling-12943S), amyloid-β (MOAB-2, 1:500, mouse host, monoclonal 6C3, Millipore-MABN254), Gr-1 (Ly-6G/Ly-6C monoclonal antibody, 1:200, rat host, Invitrogen), ionized calcium-binding adapter molecule-1 (Iba-1, 1:500, rabbit, Fujifilm Wako-019-19741), iNOs (1:200, rat, Invitrogen eBioscience), Arg-1 (1:500, goat, Abcam-ab60176), anti-choline acetyltransferase (1:500, ChAT, goat, Millipore-sigma-AB144P), cleaved caspase-3 (cleaved-caspase-3, 1:500, rabbit, Cell Signaling-9661) antibody, CD68 (1:500, mouse, Santa Cruz Biotechnology-70761), and claudin-5 (1:500, mouse, Santa Cruz Biotechnology, sc-374221). The sections were then incubated with appropriate secondary antibodies (Alexa Fluor 488, 568, or 594; Invitrogen) compatible with the aforementioned primary antibodies, followed by the incubation with DAPI (1:10,000 dilution). A total of three to four sections of brain per slide from each of five to eight mice per group were used for the histological study. Co-stained (yellow-colored) cells by two protein/peptide biomarkers (green-colored and red-colored) were quantified by cell counting per field in 20x zstack image or Pearson's

 doi:10.20944/preprints202407.0723.v

coefficients in 10x image per field obtained in ImageJ analysis (1.54J National Institutes of Health, Bethesda, MD).

2.5. Image Quantification

After immunofluorescence staining, fluorescent images were captured on ECHO Revolve fluorescent microscope using 4X, 10X, 20X, and 40X objectives, and mean intensity of fluorescence, number of immunoreactive cells, were quantified using the ImageJ software. The results were expressed in mean fluorescence intensity (MFI) per field in 10x image as we conducted previously [42]. The counting of co-localized immune-positive cells for two markers was performed manually using the cell counter application of ImageJ. The researchers performed the study blindly.

2.6. Thioflavin S Staining and Analysis of Plaques

Thioflavin S (Sigma-Aldrich, T1892) serves as a fluorescent dye for the detection of Aβ plaques in brain tissue [43]. The thioflavin S stained Aβ plaques appear bright green under fluorescence microscopy. Briefly, brain sections (20 μm thickness) were incubated in 1% thioflavin S solution in deionized water for 10 min, washed with running water carefully for 5 min, then incubated in 1% acetic acid for 15 min and rinsed again. The slides were dried by placing them on paper towels for few minutes and then dehydrated in 70%, 80%, 95%, 100% ethanol sequentially, transferred to xylene, and then mounted with Permount mounting medium and dried overnight in the dark. Thioflavin-S-positive plaques were determined from the images taken by Discover-ECHO Revolve fluorescence microscope in a single plain at 4× magnification. The images were subjected to threshold processing (Otsu) using ImageJ, and the total number of plaques based on size (less than and greater than 100 μm) were analyzed in the cortical and hippocampal regions. For each animal, 6 fields from the cortex and from the hippocampus were imaged and analyzed.

2.7. Statistical Analysis

Results were mean ± standard error of mean (SEM). Kruskal–Wallis one-way analysis of variance (ANOVA, non-parametric test) followed by Tukey's multiple comparison post-hoc test was used to determine the statistical significance of differences between mouse groups of wildtype, 5xFAD, and 5xFAD + MarL1 (*$p < 0.05$, **$p < 0.01$, and ***$p < 0.001$). For all experiments at least three replicates were performed. The definition of the significance for various p values are described in the figure legends, together with the number of biological replicates (n) for each experiment. GraphPad Prism 9.0 (GraphPad, Boston, MA) was used for graphs and statistical analyses.

3. Results

3.1. Maresin-like1 Reduced Aβ Overload and Curbed Neuronal Population Loss in Brain Hippocampi of 5xFAD Mice

Amyloid beta deposition is most prominent in the hippocampus and cortex in the brain, especially in 5xFAD mice, as the Aβ deposition starts as early as 2 months of age [15,44]. Here, we examined the effect of long-term intranasal instillation of MarL1 on Aβ deposition and neuronal population in the hippocampus of 5xFAD mouse brains. We found a significantly more Aβ plaques in the hippocampus of the 5xAD mice than in the same brain regions in the wildtype mice (Figure 1, $p < 0.001$), and significant fewer $A\beta_{1\text{-}42}$ plaques in the MarL1-treated 5xFAD mice than in the untreated 5xFAD mice (Figure 1, $p < 0.001$). We also evaluated the cerebral plaque in hippocampal and cortical sections by staining them with thioflavin-S (Thio-S) dye that detects the β-pleated sheet of the amyloid plaques [43]. The level of plaque deposition was quantified in the hippocampus and cortex by determining the number of plaques of size > 100 μm^2 and size < 100 μm^2 [45–47]. We found a markedly greater number of plaques in the cortex and hippocampus of 5xFAD mice than in the wildtype mice (Figure S1). The numbers of plaques of each size category were markedly lower in both cortex and hippocampus of the MarL1-treated 5xFAD mice than in the same brain regions in the

 doi:10.20944/preprints202407.0723.v

vehicle treated 5xFAD mice (Figure S1, $p < 0.001$). We found that Iba-1$^+$ microglia engulfed the Aβ plaques and that those microglial cells formed clusters near Aβ plaques in 5xFAD mice (Figure S2).

We also examined Aβ-related neuronal losses by co-staining brain sections with MOAB-2 and with NeuN antibody. The NeuN$^+$ neuronal population was significantly lower in the 5xFAD mice than in the wildtype mice (Figure 1B, $p < 0.001$). MarL1 treatment rescued the NeuN$^+$ neuronal population in hippocampus (Figure 1B, $p < 0.001$), suggesting that MarL1 had a neuroprotective effect against AD pathogenesis in the brains of 5xFAD mice.

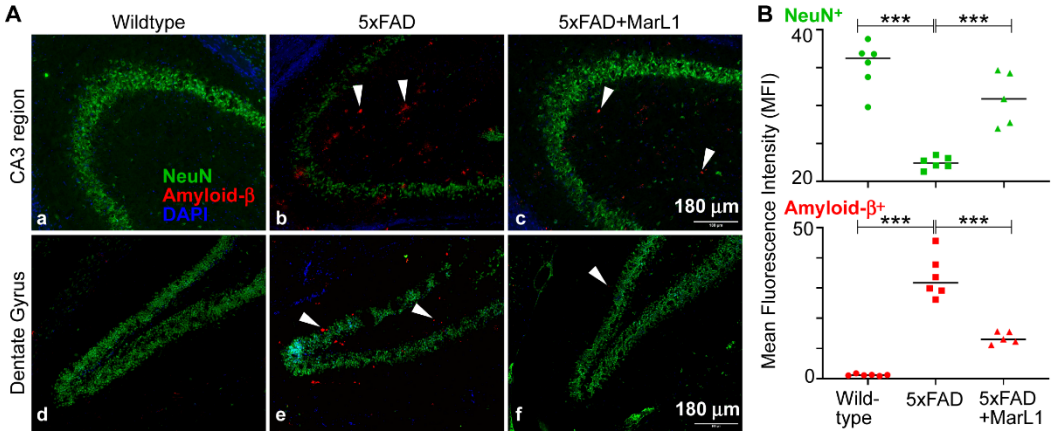

Figure 1. MarL1 treatment ameliorated AD neuropathology in brains of 5xFAD mice. (A) Immunostaining of NeuN (green) and Amyloid-β$_{1\text{-}42}$ (red) in CA3 and dentate gyrus (DG) of hippocampus. White arrows mark some Aβ$_{1\text{-}42}$ deposition in hippocampal regions. Panels a-f: 10X magnification; Scale bar: 180 μm. (B) Quantification of NeuN$^+$ and Amyloid-β$_{1\text{-}42}^+$ staining intensities of hippocampus (Mean fluorescence intensity, MFI). Data are Means ± SEM. n = 5 or 6. ***$p < 0.001$.

3.2. Maresin-like 1 Treatment of 5xFAD Mice Improved the Survival of Cholinergic Neurons and Decreased Cleaved-Caspase-3-Mediated Apoptotic Degeneration

Cholinergic neurons play the crucial roles on maintaining normal cognitive function through the neurotransmitter acetylcholine (Ach) [48]. These neurons broadly distribute throughout the brain. Striatum is one of the main areas where cholinergic neurons are found [49]. Striatum has the greatest levels of ACh in the brain [50,51]. The loss, degeneration, or dysfunction of cholinergic neurons in the brain leads to cognitive deterioration, a characteristic feature of AD [52,53].

Here, we investigated whether MarL1 treatment could curb the AD-associated decline in the cholinergic neuronal population in 5xFAD mice. We immunostained striatal brain sections with an antibody specific for choline acetyltransferase (ChAT), an enzyme that catalyzes the synthesis of acetylcholine at cholinergic synapses, thus selectively marks cholinergic neurons [54,55]. We conducted the ChAT immunostaining together with cleaved-caspase-3 antibody to quantify the apoptotic ChAT$^+$ neuronal population in the brain (Figure 2A). We found that the ChAT$^+$ neuronal population was significantly smaller in the 5xFAD mice than in their wildtype littermates ($p < 0.001$), whereas MarL1 treatment significantly inhibited this decline in the ChAT$^+$ population in 5xFAD mice compared to vehicle-treated 5xFAD mice ($p < 0.001$) (Figure 2B) in the striatum region. The number of apoptotic cleaved-caspase-3$^+$ cells was also lower in the striatum region of 5xFAD mice treated with MarL1 than with vehicle (Figure 2B, $p < 0.001$), suggesting that MarL1 treatment may be effective in protecting cholinergic neurons from apoptosis and restoring their population in the brains of 5xFAD mice.

 doi:10.20944/preprints202407.0723.v

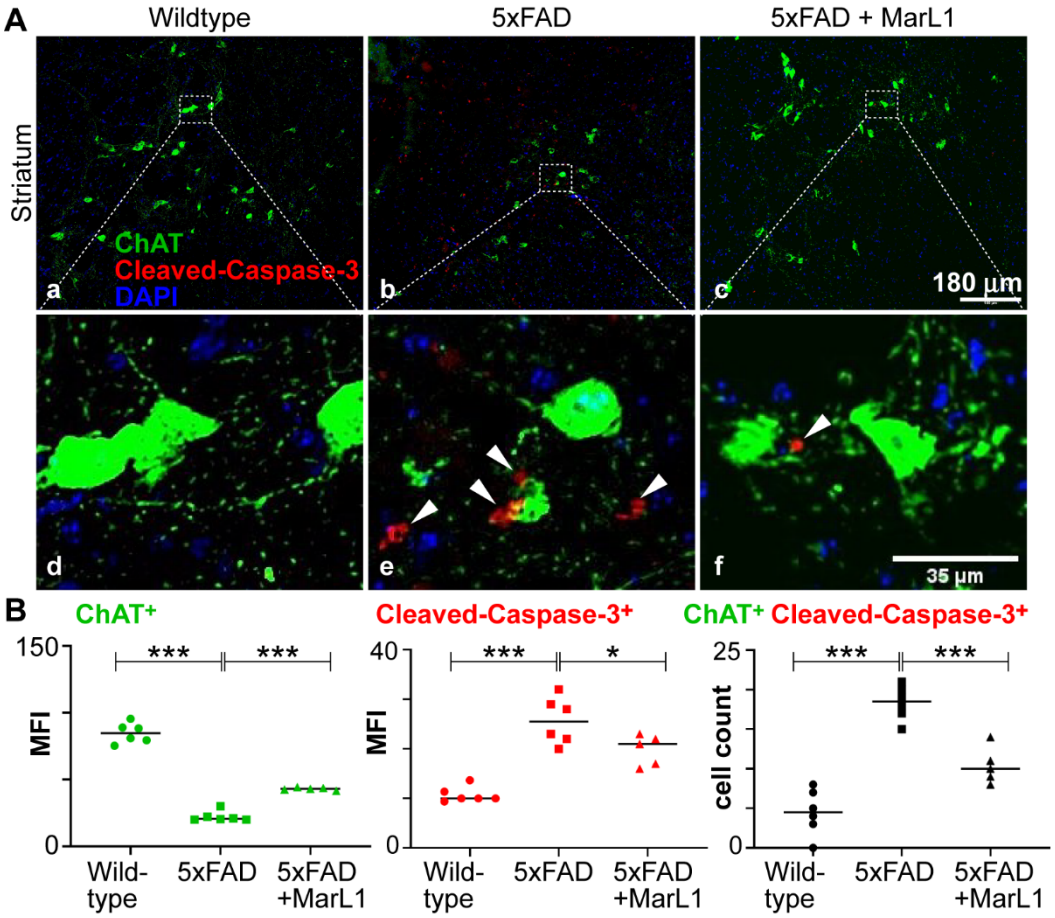

Figure 2. MarL1 protected cholinergic neurons (ChAT$^+$) and inhibited apoptotic cleaved-caspase-3 activity in brains of 5xFAD mice. (A) Immunostaining of ChAT (green) and cleaved-caspase-3 (red) in striatum (Panels a-c: 10X magnification; scale bar: 180 µm. White arrows mark cleaved-caspase-3$^+$ cholinergic neurons in zoomed-in images (Panels d-f). Scale bar: 35 µm. (B) Quantification of ChAT and caspase-3 in striatum. Left: Mean fluorescence intensity MFI for ChAT$^+$; middle: MFI for cleaved-caspase-3$^+$; right: count of cells stained positive for both ChAT and cleaved-caspase-3. Data are Means ± SEM. n = 5 or 6. *** $p < 0.001$, and *$p < 0.05$.

3.3. Maresin-like1 Attenuated the Pro-Inflammatory M1 Phenotypic Switching of Microglia by Inhibiting Iba-1$^+$CD68$^+$ Microglia in Brains of 5xFAD Mice

We investigated the effect of MarL1 on M1 phenotypic switching of microglia in brains of 5xFAD mice by immunohistological assessment of the microglial phenotype using the markers Iba-1 and CD68 for M1 microglia [23,56–58] in the brain (Figure 3A). Significantly greater immunoreactivities of Iba-1 were found in 5xFAD mice than in wildtype mice in hippocampus region (Figure 3B, $p <$ 0.001), while the immunoreactivities of Iba-1 were significantly lower in MarL1-treated mice than in vehicle-treated 5xFAD mice (Figure 3B, $p < 0.001$).

 doi:10.20944/preprints202407.0723.v

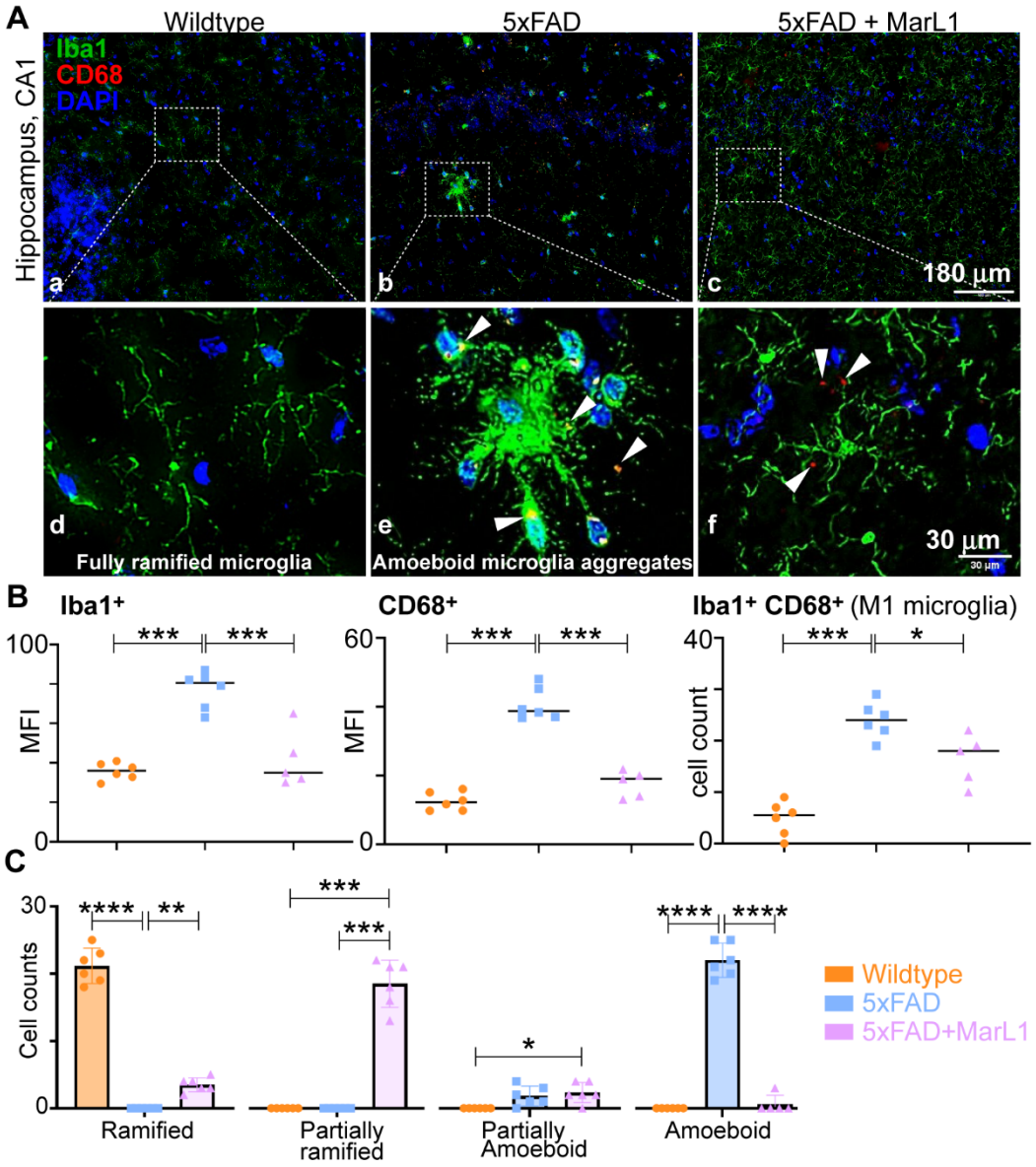

Figure 3. MarL1 suppressed pro-inflammatory M1 phenotype polarization of microglia in brains of 5xFAD mice. (A) Immunostaining of microglia with Iba-1 (green) and CD68 (red) in CA1 region of hippocampus from 5xFAD transgenic mice (Panels a-c: 10X magnification; scale bar: 180 µm. Panels d-f: zoomed-in images; scale bar: 30 µm). White arrows mark Iba-1$^+$CD68$^+$ microglia. (B) Quantification of Iba-1$^+$ and CD68$^+$ in hippocampus. Left: mean fluorescence intensity MFI of Iba-1$^+$; middle: MFI of CD68$^+$; right: count of microglia stained positive for both Iba-1$^+$ and CD68$^+$; (C) Quantification of microglia based on phenotype characterization (ramified, partially ramified, partially amoeboid, amoeboid) in hippocampus. Data are Means ± SEM. n = 5 or 6. *** $p < 0.001$, ** $p < 0.01$, and * $p < 0.05$.

We also quantified the levels of CD68 (scavenger receptor Class D), a phagocytic microglial marker on Iba-1$^+$ microglial cells, in co-stained brain coronal sections [59]. The activation of CD68$^+$ microglial cells was 3.25-fold higher in 5xFAD mice than in their wildtype littermates (Figure 3B, middle panel, $p < 0.001$), but this activation was significantly attenuated by 57% in the MarL1-treated 5xFAD mice (Figure 3B, middle panel, $p < 0.001$). The Iba-1$^+$CD68$^+$ cell count was significantly higher in 5xFAD brains than in wildtype controls (Figure 3B, right panel, $p < 0.001$), and was significantly lower in MarL1-treated 5xFAD mice than in vehicle-treated 5xFAD mice (Figure 3B, right panel, $p < 0.05$).

 doi:10.20944/preprints202407.0723.v

Microglia can be phenotypically categorized based on their circularity (i.e., the length of their processes) into different stages of activation ranging from ramified microglia (microglia at the resting stage, S0) to amoeboid microglia (microglia at the activated-stage, S1). Inter-stages also exist between S0 and S1 in the form of partially ramified microglia (having fewer processes) and partially amoeboid microglia (having 1-2 processes with a round shape) [60–62]. Notably, we observed an unusual phenomenon in the microglial phenotype in 5xFAD mice. We found that the microglial cells aggregated in the hippocampus and cortex to form a "cluster of cells" similar to those found near Aβ plaques and those microglia were partially or fully amoeboid in shape in the 5xFAD mice but did not show this morphology in the wildtype mice. We also observed some microglial aggregates in the cortex, but not in the hippocampus, of the MarL1-treated 5xFAD mice. The MarL1 treatment group showed more partially ramified microglial phenotypes than the vehicle-treated 5xFAD mice (Figure 3A).

We also quantified the numbers of microglial cells based on the morphology observed in Iba-1–immunostained sections. The number of ramified microglia was greater in the wildtype mice than in the 5xFAD and MarL1-treated mice (Figure 3C). The number of partially ramified microglia was significantly higher in the MarL1-treated 5xFAD mice than in the vehicle-treated 5xFAD or wildtype mice (Figure 3C, $p < 0.001$). The number of amoeboid microglia was significantly higher in the vehicle-treated 5xFAD mice than in the wildtype (Figure 3C, $p < 0.001$) and MarL1-treated 5xFAD mice (Figure 3C, $p < 0.001$). These results suggested that the transition of microglia from the ramified (S0) morphology to activated amoeboid (S1) morphology was greater in the 5xFAD mice than in the wildtype mice, while treatment with MarL1 attenuated that morphological transition.

3.4. Maresin-like 1 Curbed the AD Pathogenesis-Associated Decline in the M2 Microglial Population with an Anti-Inflammatory Alternatively Activated Phenotype in Brains of 5xFAD Mice

We determined the effect of MarL1 on the microglial phenotypic switch between M1 and M2 by investigating the M2 population in cortical brain sections. Immunostaining brain sections with Iba-1 and Arg-1, a biomarker for M2 microglia [63] (Figure 4A), revealed a significantly higher mean fluorescence intensity for Arg-1 in the brains of wildtype mice than of 5xFAD mice (Figure 4B, $p < 0.001$), but the population was significantly greater in MarL1-treated 5xFAD mice than in vehicle-treated 5xFAD mice; that is, the MarL1 treatment significantly restored the $Arg1^{+}Iba\text{-}1^{+}$ microglial population in 5xFAD mice (Figure 4B, $p < 0.001$). These results suggest that MarL1 treatment significantly shifted the polarization of the microglial population from M1 to M2, suggesting that MarL1 has a capacity for resolution of inflammation that could contribute to curbing AD pathogenesis.

 doi:10.20944/preprints202407.0723.v

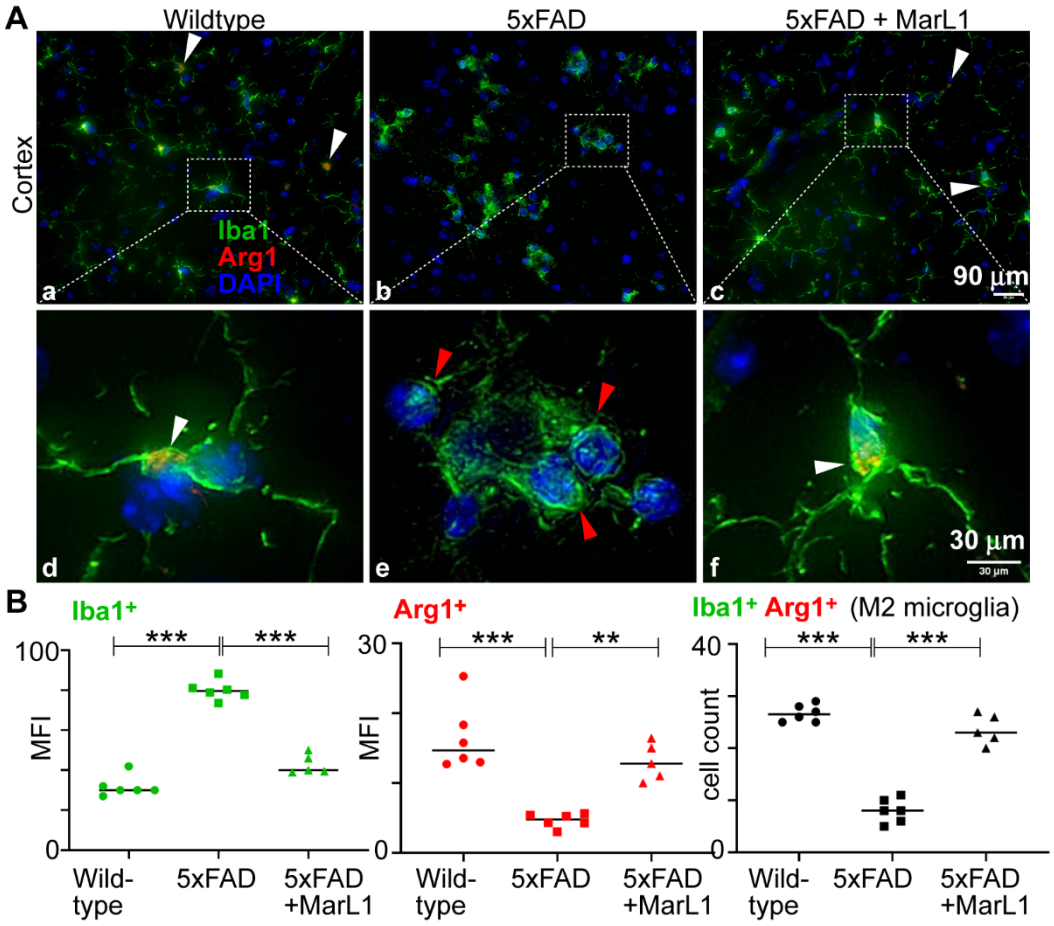

Figure 4. MarL1 promoted anti-inflammatory M2 phenotype polarization of microglia in brains of 5xFAD mice. (A) Immunostaining of microglia with Iba-1 (green) and Arg1 (red) in cortex (Panels a-c: 20X magnification; scale bar: 90 µm. Panels d-f: zoomed-in images; scale bar: 30 µm). White arrows mark Iba1⁺Arg1⁺ microglia. Red arrows mark microglial aggregation in cortex of 5xFAD mice. (B) Quantification of Iba-1 and Arg1 in cortex. Left: mean fluorescence intensity MFI of Iba1⁺; middle: MFI of Arg1⁺; right: count of microglia stained positive for both Iba1 and Arg1 in cortex. Data are Means ± SEM. n = 5 or 6. *** $p < 0.001$, and ** $p < 0.01$.

3.5. Maresin-like1 Treatment Promoted the Expression of BBB-Associated Tight-Junction Protein Claudin-5, Decreased Infiltration of Neutrophils in 5xFAD Brains, and Induced the Switch of Neutrophils toward the Inflammation-Resolving N2 Phenotype

Conventionally, AD has been viewed mainly as a neurodegenerative disorder. However, new reports suggest that dysfunction of the blood-brain barriers links to neuroinflammation of brains, which in close association with peripheral inflammatory signals, also play a significant role in AD [29–31,64,65]. Patients with early cognitive decline or mild cognitive impairment have been reported to show BBB breakdown in the hippocampus (CA1, CA3, and dentate gyrus) and parahippocampal gyrus, area crucial for memory and learning [66]. As a result, the BBB can no longer effectively clear Aβ, and that Aβ then accumulates in the brain and blood vessels [67,68], leading to increased expression of adhesion molecules on brain blood vessels and the release of inflammatory substances that potentially promote leukocyte recruitment [67].

When activated, resident immune cells in brains, such as microglia, can release tissue danger signals, cytokines, and chemokines that recruit leukocytes from the peripheral circulation to inflamed areas in brains. Both experimental and clinical evidence shows that neutrophils and T-cells migrate into the brain in AD [69–72]. The study using two-photon laser scanning microscopy revealed that vascular deposition of Aβ in brains of 5xFAD mice facilitates intraluminal adherence and movement

 doi:10.20944/preprints202407.0723.v

of neutrophils in brain blood vessels [34,73]. Neutrophils were discovered to selectively leak into the parenchyma of the regions with Aβ deposits. [34,73]. We explored the possibility of neutrophil infiltration in the brain by immunostaining cortical sections with Gr-1 (a marker for myeloid differentiation, present primarily in neutrophils and transiently in monocytes/macrophages) and claudin-5 (a tight-junction protein present in endothelial cells of vessels in brain for vasculature), as shown in Figure 5A. We found a significantly greater influx of neutrophils in 5xFAD mice than in wildtype mice (Figure 5B, $p < 0.001$). The MarL1 treatment significantly reduced this influx compared to vehicle-treated 5xFAD mice (Figure 5B, $p < 0.001$). We also observed a phenomenon called "neutrophil swarming" in 5xFAD mice, which is the accumulation of large numbers of neutrophils to neutralize large microbes and clusters of microbes in a targeted region [74,75]. Here, we noticed a massive number of neutrophil aggregations in the cortex of 5xFAD mice brain. One possibility is that neutrophil swarming may occur due to the presence of Aβ plaques in the cortex of 5xFAD mice. Here, we report the first evidence for "neutrophil swarming" in the cortex of the brains of 5xFAD mice. We did not observe neutrophil swarming in MarL1-treated 5xFAD mice, although the neutrophil clusters that are not swarming were evident in the cortical sections (Figure 5A).

The BBB integrity was further assessed using the tight-junction protein marker claudin-5, which is critical for preserving the integrity of the endothelial cells of brain blood vessels, and staining endothelial cells in the blood vessels in the brain [76]. The mean claudin-5 intensities were significantly lower in 5xFAD mice than in wildtype mice. The MarL1 treatment restored the BBB integrity by increasing the claudin-5 levels in brain blood vessels in 5xFAD mice (Figure 5B). These results suggest that MarL1 treatment may provide a protective effect on the BBB integrity and decrease the infiltration of immune cells into the brain.

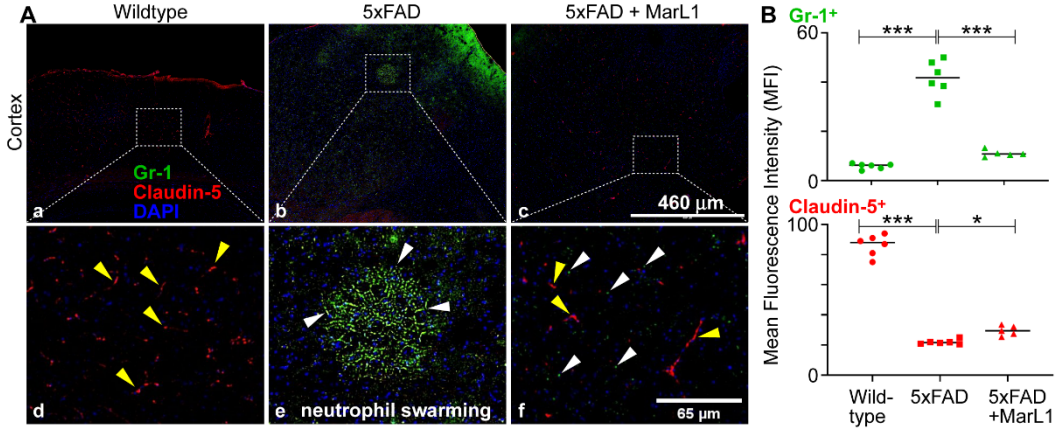

Figure 5. MarL1 attenuated the AD-associated compromise of blood–brain-barrier tight-junctions as well as neutrophil infiltration into brains of 5xFAD mice. (A) Immunostaining of Gr-1 (green) for neutrophils and Claudin-5 (red) for tight-junctions of the vasculatures in cortex. Panels a-c show images from cortex (4X magnification; scale bar: 460 µm). Panels d-f show zoomed-in images; scale bar: 65 µm. White arrows mark some Gr-1$^+$ cells outside the vasculature in parenchyma in zoomed-in images. Yellow arrows mark some claudin-5$^+$ vasculatures. Neutrophil swarming is evident in panels b and e. (B) Quantification of Gr-1$^+$ and Claudin-5$^+$ in MFI in cortex. Data are Means ± SEM. n = 5 or 6. *** $p < 0.001$, and *$p < 0.05$.

We also categorized the infiltrating neutrophil population into N1-neutrophils, a pro-inflammatory phenotype [35], and N2-neutrophils, anti-inflammatory phenotype of pro-resolution of inflammation [36]. Immunostaining of coronal brain sections using the co-localization of Gr-1 and iNOS (Gr-1$^+$iNOS$^+$) revealed more Gr-1$^+$iNOS$^+$ N1 neutrophils in 5xFAD mice than in wildtype mice (Figure 6A), while MarL1 treatment reversed this trend in the hippocampal region. The Pearson's coefficients between the mean fluorescence intensities, MFIs of Gr-1$^+$ cells and iNOS$^+$ cells are consistent with this trend about the co-localization Gr-1$^+$ and iNOS$^+$ (Figure 6B right panel, $p < 0.01$ or 0.05). By contrast, the microimages of Gr-1 and Arg1 co-localized brain sections showed less N2 neutrophils in 5xFAD mice than in wildtype mice (Figure 7A) and MarL1 treatment replenished the

 doi:10.20944/preprints202407.0723.v

N2 population above that in vehicle-treated 5xFAD mice. This direct microscopic observation is consistent with the analysis of Pearson's coefficients between MFIs of Gr-1⁺ cells and Arg1⁺ cells in the microimages (Figure 7B right panel, $p < 0.001$ or 0.01). These results suggest that MarL1 treatment polarizes the shift of N1 to N2 neutrophil population in neurodegenerative events.

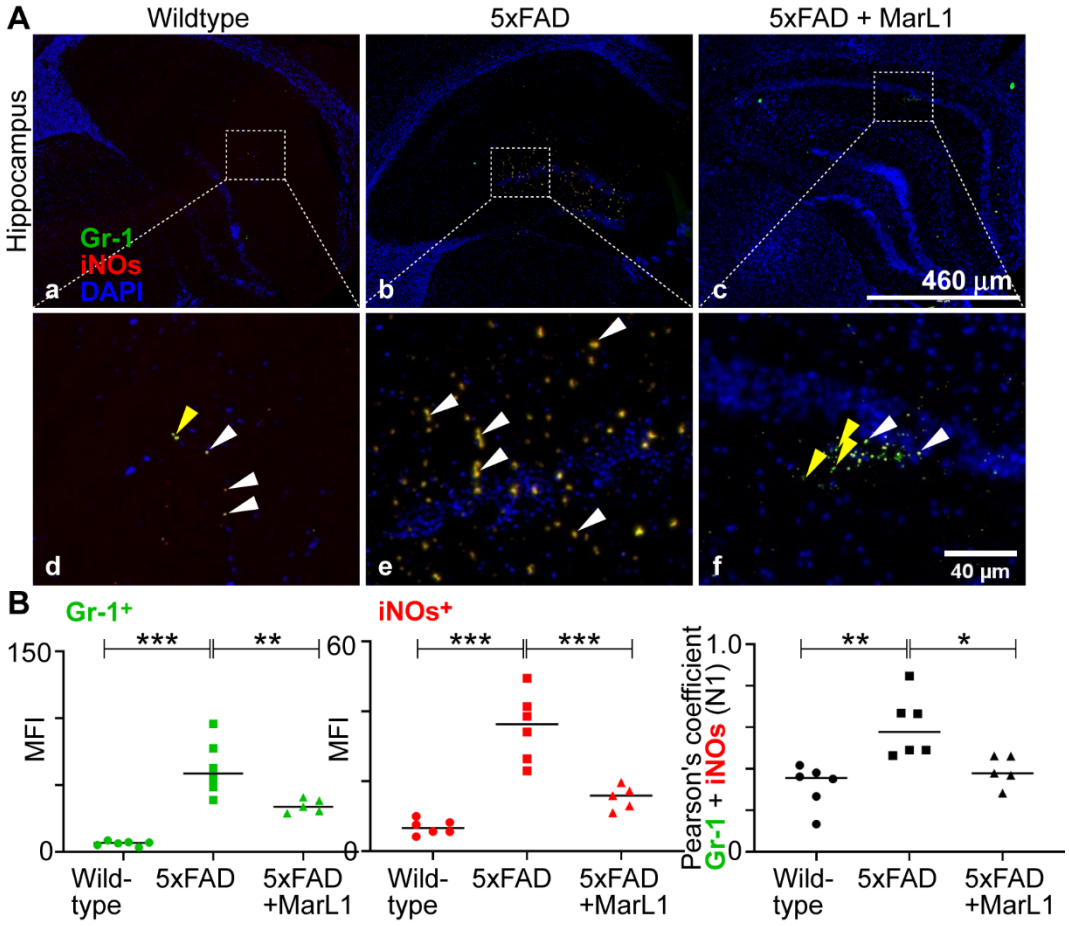

Figure 6. MarL1 treatment suppressed pro-inflammatory N1 polarization of neutrophils infiltrated into AD-pathogenic brains in 5xFAD mice. (A) Immunostaining of Gr-1 (green) for neutrophils and iNOs (red), an inflammatory marker. Panels a-c show hippocampus (4X magnification, scale bar: 460 µm). Panels d-f show zoomed-in images; scale bar: 40 µm. White arrows mark some Gr-1⁺iNOs⁺ cells and yellow arrows mark only Gr-1 positive cells in zoomed-in panels. (B) Quantification of Gr-1⁺ and iNOs⁺ in hippocampus. Left: MFI of Gr-1⁺; middle: MFI of iNOs⁺; right: Pearson's coefficient for quantification of co-localization of Gr-1 and iNOs. Data are Means ± SEM. n = 5 or 6. *** $p < 0.001$, ** $p < 0.01$, and * $p < 0.05$.

 doi:10.20944/preprints202407.0723.v

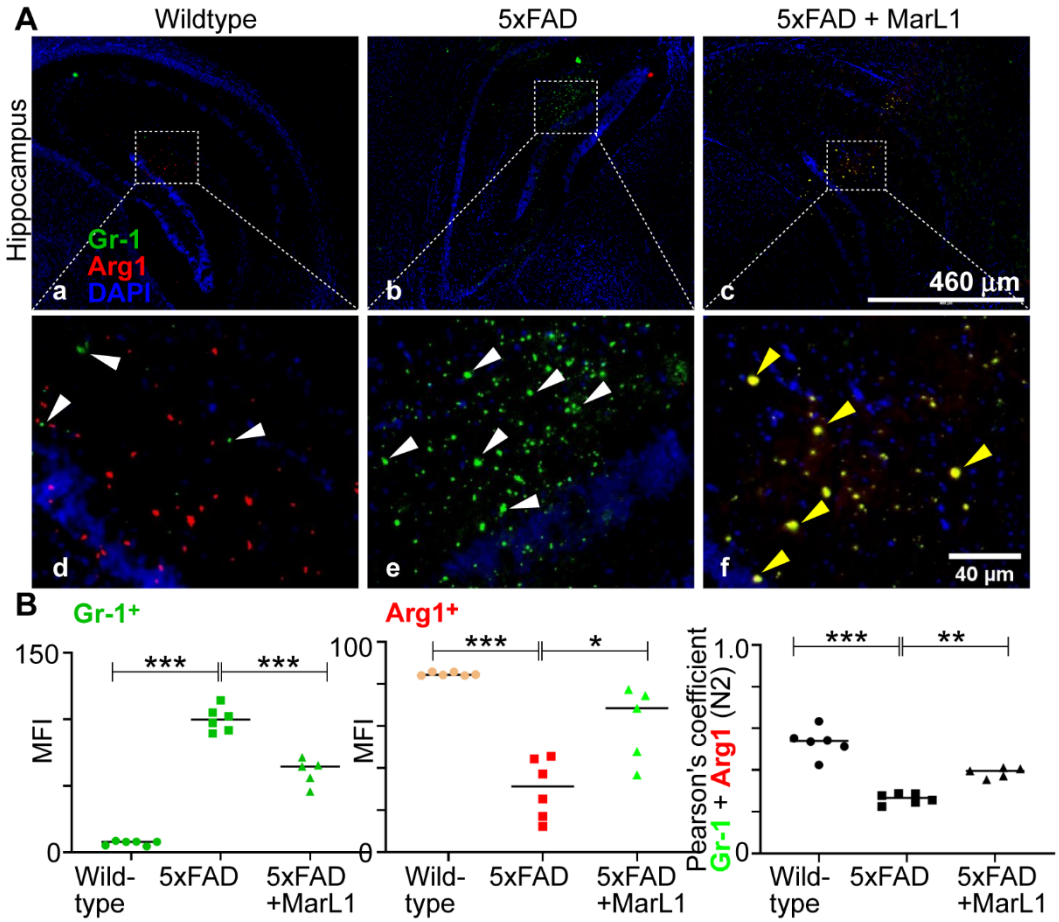

Figure 7. MarL1 treatment induced anti-inflammatory N2 phenotypic polarization of neutrophils infiltrated into AD-pathogenic brains in 5xFAD mice. (A) Immunostaining of Gr-1 (green) for neutrophils and Arg1(red), an anti-inflammatory marker. Panels a-c show hippocampus (4X magnification, scale bar: 460 µm). Panels d-f show zoomed-in images; scale bar: 40 µm. White arrows mark Gr-1$^+$ cells and yellow arrows mark Gr-1$^+$Arg1$^+$ cells in zoomed-in panels. (B) Quantification of Gr-1$^+$ and Arg1$^+$ in hippocampus. Left: MFI of Gr-1$^+$; middle: MFI of Arg1$^+$; right: Pearson's coefficient for quantification of co-localization of Gr-1 and Arg1. Data are Means ± SEM. n = 5 or 6. *** $p < 0.001$, ** $p < 0.01$, and *$p < 0.05$.

4. Discussion

Neuroinflammation is pivotal in the development of AD, as it can worsen Aβ and Tau pathologies [77–79]. In the present study, we examined the effect of MarL1 on the extent of inflammation in brains of transgenic 5xFAD mice.

We evaluated the effect of intranasal instillation of the MarL1 mediator from the age of 1.5 to 9 months in 5xFAD mice. Intranasal instillation of drugs is well recognized to partly bypass the BBB to deliver drugs to brains more efficiently than *ip* or *iv* methods, thereby increasing drug bioavailability in the brain, while also delivering drugs noninvasively and to the blood circulation as well [39,80–82]. At the age of 12.5 months, 5xFAD mice show a significant reduction in levels of oligomeric Aβ42 and Aβ plaques in cortex and hippocampal regions of the brain and in the loss of NeuN$^+$ neurons in CA3 and dentate gyrus regions of hippocampus under MarL1 treatment (Figure 1). Quantification of the Aβ plaque numbers based on sizes greater than and less than 100 µm^2 area [45–47] using thioflavin-S staining revealed a marked reduction in the number of Aβ plaques following MarL1 treatment of 5xFAD mice (Figure S1). The neuroprotective effect of MarL1 was mediated by restoring the cholinergic neurons in striatum and decreasing the apoptotic cleaved caspase-3$^+$ neurons in brain. Other studies have shown increased activation of cleaved caspase-3 in the hippocampus of AD

 doi:10.20944/preprints202407.0723.v

patients and increases in the levels of synaptic pro-caspase-3 and cleaved caspase-3 in the postsynaptic density fractions [83]. These findings suggest that MarL1 has a neuroprotective effect in the brain.

Neuroinflammation plays a vital role in neurodegeneration by contributing to neuronal damage and synaptic loss, with microglia as the key players [84–86]. Histological examinations of AD brains show that microglial cells are found in close association with Aβ deposits, especially dense-core plaques [87–89]. The quantity of microglia increases proportionally with plaque dimension [90]. Aβ deposition has been reported to attract a microglial cells, resulting in their accumulation at the periphery of the plaque [87]. Our results demonstrate enhanced microglial phagocytosis of Aβ plaques (Figure S2), and we found microglia in clusters in 5xFAD mice. These aggregates showed that microglial accumulation and proliferation in the brain could cause neuroinflammation, while MarL1 treatment reduced the Aβ accumulation thereby decreasing the microglial activation.

Enhanced microglial activation leads to increases in the expression of pro-inflammatory markers, including interleukin-1β, TNF-α, and iNOs, which in turn promote neuroinflammation [91,92]. Our data demonstrate that MarL1 treatment attenuated microglial activation by decreasing the population of Iba-1$^+$ microglia and CD68 expression in the hippocampus (CA1, dentate gyrus) of the 5xFAD mouse brain. We phenotypically characterized microglia and calculated the number of microglia in different states as: 1) ramified, 2) partially- ramified, 3) partially-amoeboid, 4) and fully-amoeboid microglia [93,94]. We found that MarL1 reduced the level of amoeboid microglia, suggesting its inflammation-resolving and anti-inflammatory properties are a consequence of suppression of microglial activation (Figure 3).

Specialized pro-resolving lipid mediators are reported to modulate immunity and inflammation by resolving inflammation by triggering a biochemical paradigm shift commonly referred to as the "lipid mediator class switch" and skewing the M1/M2 macrophage balance toward the anti-inflammatory M2 phenotype, with replacement of injured cells and restoration of the normal functions of tissues [6]. Consistent with these reports, MarL1 treatment caused a shift in the M1/M2 population in brain as indicated by a surging Arg-1$^+$ microglial population in the brain (Figure 4). These finding suggest that MarL1 is an effective immunoresolvent in brains

In this study we explored the concept of neutrophil migration in brain parenchyma. Here, we observed the phenomenon of "neutrophil swarming" [95] in the cortex, as shown in Figure 5, representing neutrophil aggregation in the 5xFAD mouse brain. This is the first immunohistochemical report of neutrophil swarming in the brain cortex in the literature. Co-saining of Gr-1 (a marker for neutrophils) and claudin-5 (a marker for vasculature) showed that Gr-1$^+$ neutrophils migrated into the brain and formed swarms, as neutrophils are nonresident cells in brains. We could not find neutrophil swarms in the brains of MarL1-treated 5xFAD mice, although neutrophils aggregate was evident than wildtype mice. No swarms were detected in the brains of the wildtype littermates. These findings suggests that neutrophil infiltration into brains could contribute to AD pathogenesis since neutrophils produce reactive oxygen species and degradation enzymes that can cause neuroinflammation and neurodegeneration [34,73,96]. Furthermore, our findings revealed that MarL1 treatment inhibited the AD-linked neutrophil infiltration and swarm in the brains of 5xFAD mice.

Neutrophils play significant roles in the pathogenesis of AD and is categorized into pro-inflammatory N1 [35] and anti-inflammatory N2 subpopulations [36]. In our study, we found that Gr-1$^+$iNOS$^+$ N1 neutrophils increased in 5xFAD mice. We also found that MarL1 treatment dampens the elevation of N1 neutrophils in brain (Figure 6). Furthermore, Gr-1$^+$Arg1$^+$ N2 neutrophils were amplified with MarL1 treatment and were lower in 5xFAD mice than in wildtype controls (Figure 7). These results demonstrate that chronic MarL1 treatment polarizes a shift from N1 to N2 in 5xFAD mice, suggesting resolution of inflammation in the brain.

Taken together, our results provide the first evidence that MarL1 was effective in inhibiting Aβ pathology in brain. However, the 5xFAD mouse model is an aggressive early onset transgenic AD model [16,97–100], therefore, the protection effects of MarL1 need to be explored using less aggressive AD models, including late-onset AD models [100,101]. Furthermore, the different doses of MarL1 and

 doi:10.20944/preprints202407.0723.v

their safety should be evaluated for future clinical studies. Further research is needed to fully understand the mechanisms involved in the neuroprotection imparted by MarL1 in AD. MarL1-specific receptor targeted research could be a promising strategy for developing new treatments for this debilitating disease.

5. Conclusions

The long-term administration of MarL1 in 5xFAD mice had a positive impact on reducing the neuropathology associated with Alzheimer's disease in the brains of 5xFAD mice—an animal model deemed appropriate for the study of early onset AD and Aβ pathology. This study highlights the potential use of MarL1 as a therapeutic lead for the treatment of AD as shown in Figure 8. Further research is needed to fully understand the underlying mechanisms of action and to further optimize the treatment efficacy. MarL1 treatment efficiency and its involved mechanisms should also be studied using the animal models available for AD Tau pathology.

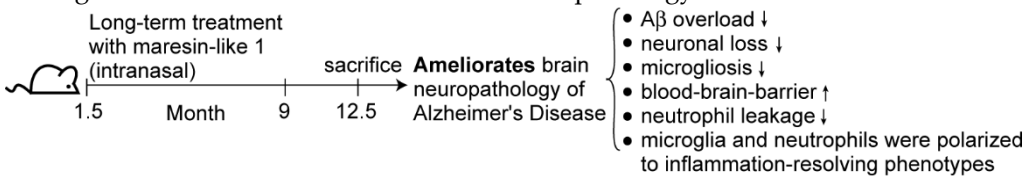

Figure 8. A graphic summary.

Supplementary Materials: The following supporting information can be downloaded at the website of this paper posted on Preprints.org, Figure S1: MarL1 treatment prevented or reduced the elevation of thioflavin-S positive cerebral plaques in brains of 5xFAD mice; Figure S2: The interaction between microglia (a-c) and amyloid beta plaques in cortex and hippocampus of 5xFAD mice.

Author Contributions: Conceptualization, S.H.; Methodology, S.H., Y.L., P.S., Y.K., Y.Z., W.L; Validation, P.S., Y.L., S.S., Y.K., Y.Z., N.L., A.-R.M. and S.H.; Formal analysis P.S., Y.L., N.L. and S.H.; Investigation, P.S., Y.L., Y.K., Y.Z., N.L. and S.H.; Resources, Y.K., Y.Z., W.L., and S.H.; Data curation, P.S., Y.L., Y.K., Y.Z., N.L. and S.H.; Writing—original draft, P.S., Y.L., S.S. and S.H.; Writing—review & editing, P.S., Y.L., S.S., Y.K., Y.Z., N.L., A.-R.M. and S.H.; Visualization, P.S., Y.L. and S.H.; Supervision: Y.K. and S.H.; Project administration, Y.K. and S.H.; Funding acquisition, Y.K. and S.H.

Funding: This research was funded by LSU Health-New Orleans research enhancement fund (to S.H.), USA National Institute of Health grants 1R21AG060430, 1R21AG066119, and 1R21AG068756 (to S.H.) and the Japan Society for the Promotion of Science JSPS KAKENHI, Grant Number JP15H05904 (to Y. K.).

Institutional Review Board Statement: The animal use protocols [#3616 (2018-2021), #3876 (2021 to present)] have been authorized and approved by the Institutional Animal Care and Use Committee of Louisiana State University, Health, New Orleans, USA.

Data Availability Statement: Data is contained within the article.

Acknowledgments: We are very grateful to Professor Nicholas G Bazan, the director of Neuroscience Center of Excellence (NCE), School of Medicine, LSU, Health-New Orleans, USA for the strong support to make this research possible.

Conflicts of Interest: The authors do not have any conflict of interest.

References

1. 2022 Alzheimer's disease facts and figures. *Alzheimers Dement* **2022**, *18*, 700-789, doi:10.1002/alz.12638.
2. Giridharan, V.V.; Barichello De Quevedo, C.E.; Petronilho, F. Microbiota-gut-brain axis in the Alzheimer's disease pathology - an overview. *Neurosci Res* **2022**, *181*, 17-21, doi:10.1016/j.neures.2022.05.003.
3. Long, J.M.; Holtzman, D.M. Alzheimer Disease: An Update on Pathobiology and Treatment Strategies. *Cell* **2019**, *179*, 312-339, doi:10.1016/j.cell.2019.09.001.
4. Hong, Y.; Xu, J.; Hu, Y.; Li, L.; Dong, Z.; Zhu, T.; Wei, Y. Neuroinflammation and Neuroimmunomodulation in Alzheimer's Disease. *Current Pharmacology Reports* **2018**, *4*, 408-413.
5. Leng, F.; Hinz, R.; Gentleman, S.; Hampshire, A.; Dani, M.; Brooks, D.J.; Edison, P. Neuroinflammation is independently associated with brain network dysfunction in Alzheimer's disease. *Molecular psychiatry* **2023**, *28*, 1303-1311, doi:10.1038/s41380-022-01878-z.

6. Chiurchiu, V.; Maccarrone, M. Bioactive lipids as modulators of immunity, inflammation and emotions. *Curr Opin Pharmacol* **2016**, *29*, 54-62, doi:10.1016/j.coph.2016.06.005.
7. Serhan, C.N.; Yang, R.; Martinod, K.; Kasuga, K.; Pillai, P.S.; Porter, T.F.; Oh, S.F.; Spite, M. Maresins: novel macrophage mediators with potent antiinflammatory and proresolving actions. *J Exp Med* **2009**, *206*, 15-23.
8. Serhan, C.N.; Dalli, J.; Karamnov, S.; Choi, A.; Park, C.K.; Xu, Z.Z.; Ji, R.R.; Zhu, M.; Petasis, N.A. Macrophage proresolving mediator maresin 1 stimulates tissue regeneration and controls pain. *Faseb J* **2012**, *26*, 1755-1765.
9. Hong, S.; Lu, Y.; Tian, H.; Alapure, B.V.; Wang, Q.; Bunnell, B.A.; Laborde, J.M. Maresin-like lipid mediators are produced by leukocytes and platelets and rescue reparative function of diabetes-impaired macrophages. *Chem Biol* **2014**, *21*, 1318-1329, doi:10.1016/j.chembiol.2014.06.010.
10. Francos-Quijorna, I.; Santos-Nogueira, E.; Gronert, K.; Sullivan, A.B.; Kopp, M.A.; Brommer, B.; David, S.; Schwab, J.M.; Lopez-Vales, R. Maresin 1 Promotes Inflammatory Resolution, Neuroprotection, and Functional Neurological Recovery After Spinal Cord Injury. *J Neurosci* **2017**, *37*, 11731-11743, doi:10.1523/JNEUROSCI.1395-17.2017.
11. Zhu, M.; Wang, X.; Hjorth, E.; Colas, R.A.; Schroeder, L.; Granholm, A.C.; Serhan, C.N.; Schultzberg, M. Pro-Resolving Lipid Mediators Improve Neuronal Survival and Increase Abeta42 Phagocytosis. *Mol Neurobiol* **2016**, *53*, 2733-2749, doi:10.1007/s12035-015-9544-0.
12. Sanchez-Fernandez, A.; Zandee, S.; Mastrogiovanni, M.; Charabati, M.; Rubbo, H.; Prat, A.; Lopez-Vales, R. Administration of Maresin-1 ameliorates the physiopathology of experimental autoimmune encephalomyelitis. *J Neuroinflammation* **2022**, *19*, 27, doi:10.1186/s12974-022-02386-1.
13. Yin, P.; Wang, X.; Wang, S.; Wei, Y.; Feng, J.; Zhu, M. Maresin 1 Improves Cognitive Decline and Ameliorates Inflammation in a Mouse Model of Alzheimer's Disease. *Front Cell Neurosci* **2019**, *13*, 466, doi:10.3389/fncel.2019.00466.
14. Emre, C.; Arroyo-Garcia, L.E.; Do, K.V.; Jun, B.; Ohshima, M.; Alcalde, S.G.; Cothern, M.L.; Maioli, S.; Nilsson, P.; Hjorth, E.; et al. Intranasal delivery of pro-resolving lipid mediators rescues memory and gamma oscillation impairment in App(NL-G-F/NL-G-F) mice. *Commun Biol* **2022**, *5*, 245, doi:10.1038/s42003-022-03169-3.
15. Oakley, H.; Cole, S.L.; Logan, S.; Maus, E.; Shao, P.; Craft, J.; Guillozet-Bongaarts, A.; Ohno, M.; Disterhoft, J.; Van Eldik, L.; et al. Intraneuronal beta-amyloid aggregates, neurodegeneration, and neuron loss in transgenic mice with five familial Alzheimer's disease mutations: potential factors in amyloid plaque formation. *J Neurosci* **2006**, *26*, 10129-10140, doi:10.1523/JNEUROSCI.1202-06.2006.
16. Oblak, A.L.; Lin, P.B.; Kotredes, K.P.; Pandey, R.S.; Garceau, D.; Williams, H.M.; Uyar, A.; O'Rourke, R.; O'Rourke, S.; Ingraham, C.; et al. Comprehensive Evaluation of the 5XFAD Mouse Model for Preclinical Testing Applications: A MODEL-AD Study. *Frontiers in aging neuroscience* **2021**, *13*, 713726, doi:10.3389/fnagi.2021.713726.
17. Guo, S.; Wang, H.; Yin, Y. Microglia Polarization From M1 to M2 in Neurodegenerative Diseases. *Frontiers in aging neuroscience* **2022**, *14*, 815347, doi:10.3389/fnagi.2022.815347.
18. Giannoni, P.; Arango-Lievano, M.; Neves, I.D.; Rousset, M.C.; Baranger, K.; Rivera, S.; Jeanneteau, F.; Claeysen, S.; Marchi, N. Cerebrovascular pathology during the progression of experimental Alzheimer's disease. *Neurobiol Dis* **2016**, *88*, 107-117, doi:10.1016/j.nbd.2016.01.001.
19. Landel, V.; Baranger, K.; Virard, I.; Loriod, B.; Khrestchatisky, M.; Rivera, S.; Benech, P.; Feron, F. Temporal gene profiling of the 5XFAD transgenic mouse model highlights the importance of microglial activation in Alzheimer's disease. *Mol Neurodegener* **2014**, *9*, 33, doi:10.1186/1750-1326-9-33.
20. Nimmerjahn, A.; Kirchhoff, F.; Helmchen, F. Resting microglial cells are highly dynamic surveillants of brain parenchyma in vivo. *Science* **2005**, *308*, 1314-1318, doi:10.1126/science.1110647.
21. Guo, Y.; Dai, W.; Zheng, Y.; Qiao, W.; Chen, W.; Peng, L.; Zhou, H.; Zhao, T.; Liu, H.; Zheng, F.; et al. Mechanism and Regulation of Microglia Polarization in Intracerebral Hemorrhage. *Molecules* **2022**, *27*, doi:10.3390/molecules27207080.
22. Wang, J.; He, W.; Zhang, J. A richer and more diverse future for microglia phenotypes. *Heliyon* **2023**, *9*, e14713, doi:10.1016/j.heliyon.2023.e14713.
23. Koizumi, T.; Taguchi, K.; Mizuta, I.; Toba, H.; Ohigashi, M.; Onishi, O.; Ikoma, K.; Miyata, S.; Nakata, T.; Tanaka, M.; et al. Transiently proliferating perivascular microglia harbor M1 type and precede cerebrovascular changes in a chronic hypertension model. *J Neuroinflammation* **2019**, *16*, 79, doi:10.1186/s12974-019-1467-7.
24. Varin, A.; Gordon, S. Alternative activation of macrophages: immune function and cellular biology. *Immunobiology* **2009**, *214*, 630-641, doi:10.1016/j.imbio.2008.11.009.
25. Martinez, F.O.; Helming, L.; Gordon, S. Alternative activation of macrophages: an immunologic functional perspective. *Annu Rev Immunol* **2009**, *27*, 451-483, doi:10.1146/annurev.immunol.021908.132532.
26. Tang, Y.; Le, W. Differential Roles of M1 and M2 Microglia in Neurodegenerative Diseases. *Mol Neurobiol* **2016**, *53*, 1181-1194, doi:10.1007/s12035-014-9070-5.

27. Jurga, A.M.; Paleczna, M.; Kuter, K.Z. Overview of General and Discriminating Markers of Differential Microglia Phenotypes. *Front Cell Neurosci* **2020**, *14*, 198, doi:10.3389/fncel.2020.00198.
28. Manda-Handzlik, A.; Demkow, U. The Brain Entangled: The Contribution of Neutrophil Extracellular Traps to the Diseases of the Central Nervous System. *Cells* **2019**, *8*, doi:10.3390/cells8121477.
29. Santos-Lima, B.; Pietronigro, E.C.; Terrabuio, E.; Zenaro, E.; Constantin, G. The role of neutrophils in the dysfunction of central nervous system barriers. *Frontiers in aging neuroscience* **2022**, *14*, 965169, doi:10.3389/fnagi.2022.965169.
30. Rossi, B.; Constantin, G.; Zenaro, E. The emerging role of neutrophils in neurodegeneration. *Immunobiology* **2020**, *225*, 151865, doi:10.1016/j.imbio.2019.10.014.
31. Rossi, B.; Santos-Lima, B.; Terrabuio, E.; Zenaro, E.; Constantin, G. Common Peripheral Immunity Mechanisms in Multiple Sclerosis and Alzheimer's Disease. *Front Immunol* **2021**, *12*, 639369, doi:10.3389/fimmu.2021.639369.
32. Smyth, L.C.D.; Murray, H.C.; Hill, M.; van Leeuwen, E.; Highet, B.; Magon, N.J.; Osanlouy, M.; Mathiesen, S.N.; Mockett, B.; Singh-Bains, M.K.; et al. Neutrophil-vascular interactions drive myeloperoxidase accumulation in the brain in Alzheimer's disease. *Acta Neuropathol Commun* **2022**, *10*, 38, doi:10.1186/s40478-022-01347-2.
33. Kong, Y.; Liu, K.; Hua, T.; Zhang, C.; Sun, B.; Guan, Y. PET Imaging of Neutrophils Infiltration in Alzheimer's Disease Transgenic Mice. *Frontiers in neurology* **2020**, *11*, 523798, doi:10.3389/fneur.2020.523798.
34. Baik, S.H.; Cha, M.Y.; Hyun, Y.M.; Cho, H.; Hamza, B.; Kim, D.K.; Han, S.H.; Choi, H.; Kim, K.H.; Moon, M.; et al. Migration of neutrophils targeting amyloid plaques in Alzheimer's disease mouse model. *Neurobiology of aging* **2014**, *35*, 1286-1292, doi:10.1016/j.neurobiolaging.2014.01.003.
35. Mihaila, A.C.; Ciortan, L.; Macarie, R.D.; Vadana, M.; Cecoltan, S.; Preda, M.B.; Hudita, A.; Gan, A.M.; Jakobsson, G.; Tucureanu, M.M.; et al. Transcriptional Profiling and Functional Analysis of N1/N2 Neutrophils Reveal an Immunomodulatory Effect of S100A9-Blockade on the Pro-Inflammatory N1 Subpopulation. *Front Immunol* **2021**, *12*, 708770, doi:10.3389/fimmu.2021.708770.
36. Cuartero, M.I.; Ballesteros, I.; Moraga, A.; Nombela, F.; Vivancos, J.; Hamilton, J.A.; Corbi, A.L.; Lizasoain, I.; Moro, M.A. N2 neutrophils, novel players in brain inflammation after stroke: modulation by the PPARgamma agonist rosiglitazone. *Stroke* **2013**, *44*, 3498-3508, doi:10.1161/STROKEAHA.113.002470.
37. Wanrooy, B.J.; Wen, S.W.; Wong, C.H. Dynamic roles of neutrophils in post-stroke neuroinflammation. *Immunol Cell Biol* **2021**, *99*, 924-935, doi:10.1111/imcb.12463.
38. Van Dam, D.; De Deyn, P.P. Animal models in the drug discovery pipeline for Alzheimer's disease. *Br J Pharmacol* **2011**, *164*, 1285-1300, doi:10.1111/j.1476-5381.2011.01299.x.
39. Southam, D.S.; Dolovich, M.; O'Byrne, P.M.; Inman, M.D. Distribution of intranasal instillations in mice: effects of volume, time, body position, and anesthesia. *Am J Physiol Lung Cell Mol Physiol* **2002**, *282*, L833-839, doi:10.1152/ajplung.00173.2001.
40. Torika, N.; Asraf, K.; Cohen, H.; Fleisher-Berkovich, S. Intranasal telmisartan ameliorates brain pathology in five familial Alzheimer's disease mice. *Brain Behav Immun* **2017**, *64*, 80-90, doi:10.1016/j.bbi.2017.04.001.
41. Xu, J.; Tao, J.; Wang, J. Design and Application in Delivery System of Intranasal Antidepressants. *Front Bioeng Biotechnol* **2020**, *8*, 626882, doi:10.3389/fbioe.2020.626882.
42. Hong, S.; Nagayach, A.; Lu, Y.; Peng, H.; Duong, Q.A.; Pham, N.B.; Vuong, C.A.; Bazan, N.G. A high fat, sugar, and salt Western diet induces motor-muscular and sensory dysfunctions and neurodegeneration in mice during aging: Ameliorative action of metformin. *CNS Neurosci Ther* **2021**, *27*, 1458-1471, doi:10.1111/cns.13726.
43. Bussiere, T.; Bard, F.; Barbour, R.; Grajeda, H.; Guido, T.; Khan, K.; Schenk, D.; Games, D.; Seubert, P.; Buttini, M. Morphological characterization of Thioflavin-S-positive amyloid plaques in transgenic Alzheimer mice and effect of passive Abeta immunotherapy on their clearance. *Am J Pathol* **2004**, *165*, 987-995, doi:10.1016/s0002-9440(10)63360-3.
44. Crouzin, N.; Baranger, K.; Cavalier, M.; Marchalant, Y.; Cohen-Solal, C.; Roman, F.S.; Khrestchatisky, M.; Rivera, S.; Feron, F.; Vignes, M. Area-specific alterations of synaptic plasticity in the 5XFAD mouse model of Alzheimer's disease: dissociation between somatosensory cortex and hippocampus. *PLoS One* **2013**, *8*, e74667, doi:10.1371/journal.pone.0074667.
45. de Sousa, D.M.B.; Benedetti, A.; Altendorfer, B.; Mrowetz, H.; Unger, M.S.; Schallmoser, K.; Aigner, L.; Kniewallner, K.M. Immune-mediated platelet depletion augments Alzheimer's disease neuropathological hallmarks in APP-PS1 mice. *Aging (Albany NY)* **2023**, *15*, 630-649, doi:10.18632/aging.204502.
46. Liu, P.; Reichl, J.H.; Rao, E.R.; McNellis, B.M.; Huang, E.S.; Hemmy, L.S.; Forster, C.L.; Kuskowski, M.A.; Borchelt, D.R.; Vassar, R.; et al. Quantitative Comparison of Dense-Core Amyloid Plaque Accumulation in Amyloid-beta Protein Precursor Transgenic Mice. *Journal of Alzheimer's disease: JAD* **2017**, *56*, 743-761, doi:10.3233/JAD-161027.
47. Wood, J.I.; Wong, E.; Joghee, R.; Balbaa, A.; Vitanova, K.S.; Stringer, K.M.; Vanshoiack, A.; Phelan, S.J.; Launchbury, F.; Desai, S.; et al. Plaque contact and unimpaired Trem2 is required for the microglial response to amyloid pathology. *Cell Rep* **2022**, *41*, 111686, doi:10.1016/j.celrep.2022.111686.

48. Chen, Z.R.; Huang, J.B.; Yang, S.L.; Hong, F.F. Role of Cholinergic Signaling in Alzheimer's Disease. *Molecules* **2022**, *27*, doi:10.3390/molecules27061816.
49. Zhou, F.M.; Wilson, C.J.; Dani, J.A. Cholinergic interneuron characteristics and nicotinic properties in the striatum. *J Neurobiol* **2002**, *53*, 590-605, doi:10.1002/neu.10150.
50. Macintosh, F.C. The distribution of acetylcholine in the peripheral and the central nervous system. *J Physiol* **1941**, *99*, 436-442, doi:10.1113/jphysiol.1941.sp003913.
51. Lim, S.A.; Kang, U.J.; McGehee, D.S. Striatal cholinergic interneuron regulation and circuit effects. *Front Synaptic Neurosci* **2014**, *6*, 22, doi:10.3389/fnsyn.2014.00022.
52. Davies, P.; Maloney, A.J. Selective loss of central cholinergic neurons in Alzheimer's disease. *Lancet* **1976**, *2*, 1403, doi:10.1016/s0140-6736(76)91936-x.
53. Mesulam, M. The cholinergic lesion of Alzheimer's disease: pivotal factor or side show? *Learn Mem* **2004**, *11*, 43-49, doi:10.1101/lm.69204.
54. Yan, H.; Pang, P.; Chen, W.; Zhu, H.; Henok, K.A.; Li, H.; Wu, Z.; Ke, X.; Wu, J.; Zhang, T.; et al. The Lesion Analysis of Cholinergic Neurons in 5XFAD Mouse Model in the Three-Dimensional Level of Whole Brain. *Mol Neurobiol* **2018**, *55*, 4115-4125, doi:10.1007/s12035-017-0621-4.
55. Saunders, A.; Granger, A.J.; Sabatini, B.L. Corelease of acetylcholine and GABA from cholinergic forebrain neurons. *Elife* **2015**, *4*, doi:10.7554/eLife.06412.
56. Kobayashi, K.; Imagama, S.; Ohgomori, T.; Hirano, K.; Uchimura, K.; Sakamoto, K.; Hirakawa, A.; Takeuchi, H.; Suzumura, A.; Ishiguro, N.; et al. Minocycline selectively inhibits M1 polarization of microglia. *Cell death & disease* **2013**, *4*, e525, doi:10.1038/cddis.2013.54.
57. Morganti, J.M.; Riparip, L.K.; Rosi, S. Call Off the Dog(ma): M1/M2 Polarization Is Concurrent following Traumatic Brain Injury. *PLoS One* **2016**, *11*, e0148001, doi:10.1371/journal.pone.0148001.
58. Hashimoto, A.; Karim, M.R.; Kuramochi, M.; Izawa, T.; Kuwamura, M.; Yamate, J. Characterization of Macrophages and Myofibroblasts Appearing in Dibutyltin Dichloride-Induced Rat Pancreatic Fibrosis. *Toxicol Pathol* **2020**, *48*, 509-523, doi:10.1177/0192623319893310.
59. Hopperton, K.E.; Mohammad, D.; Trepanier, M.O.; Giuliano, V.; Bazinet, R.P. Markers of microglia in post-mortem brain samples from patients with Alzheimer's disease: a systematic review. *Molecular psychiatry* **2018**, *23*, 177-198, doi:10.1038/mp.2017.246.
60. Sheets, K.G.; Jun, B.; Zhou, Y.; Zhu, M.; Petasis, N.A.; Gordon, W.C.; Bazan, N.G. Microglial ramification and redistribution concomitant with the attenuation of choroidal neovascularization by neuroprotectin D1. *Mol Vis* **2013**, *19*, 1747-1759.
61. Crews, F.T.; Lawrimore, C.J.; Walter, T.J.; Coleman, L.G., Jr. The role of neuroimmune signaling in alcoholism. *Neuropharmacology* **2017**, *122*, 56-73, doi:10.1016/j.neuropharm.2017.01.031.
62. Guo, L.; Choi, S.; Bikkannavar, P.; Cordeiro, M.F. Microglia: Key Players in Retinal Ageing and Neurodegeneration. *Front Cell Neurosci* **2022**, *16*, 804782, doi:10.3389/fncel.2022.804782.
63. Cherry, J.D.; Olschowka, J.A.; O'Banion, M.K. Neuroinflammation and M2 microglia: the good, the bad, and the inflamed. *J Neuroinflammation* **2014**, *11*, 98, doi:10.1186/1742-2094-11-98.
64. Morris, J.K.; Honea, R.A.; Vidoni, E.D.; Swerdlow, R.H.; Burns, J.M. Is Alzheimer's disease a systemic disease? *Biochim Biophys Acta* **2014**, *1842*, 1340-1349, doi:10.1016/j.bbadis.2014.04.012.
65. Wang, J.; Gu, B.J.; Masters, C.L.; Wang, Y.J. A systemic view of Alzheimer disease - insights from amyloid-beta metabolism beyond the brain. *Nat Rev Neurol* **2017**, *13*, 612-623, doi:10.1038/nrneurol.2017.111.
66. Nation, D.A.; Sweeney, M.D.; Montagne, A.; Sagare, A.P.; D'Orazio, L.M.; Pachicano, M.; Sepehrband, F.; Nelson, A.R.; Buennagel, D.P.; Harrington, M.G.; et al. Blood-brain barrier breakdown is an early biomarker of human cognitive dysfunction. *Nature medicine* **2019**, *25*, 270-276, doi:10.1038/s41591-018-0297-y.
67. Zlokovic, B.V. Neurovascular pathways to neurodegeneration in Alzheimer's disease and other disorders. *Nat Rev Neurosci* **2011**, *12*, 723-738, doi:10.1038/nrn3114.
68. Chen, Y.; He, Y.; Han, J.; Wei, W.; Chen, F. Blood-brain barrier dysfunction and Alzheimer's disease: associations, pathogenic mechanisms, and therapeutic potential. *Frontiers in aging neuroscience* **2023**, *15*, 1258640, doi:10.3389/fnagi.2023.1258640.
69. Zenaro, E.; Piacentino, G.; Constantin, G. The blood-brain barrier in Alzheimer's disease. *Neurobiol Dis* **2017**, *107*, 41-56, doi:10.1016/j.nbd.2016.07.007.
70. Zlokovic, B.V. The blood-brain barrier in health and chronic neurodegenerative disorders. *Neuron* **2008**, *57*, 178-201, doi:10.1016/j.neuron.2008.01.003.
71. Abbott, A. Dementia: a problem for our age. *Nature* **2011**, *475*, S2-4, doi:10.1038/475S2a.
72. Heneka, M.T.; Carson, M.J.; El Khoury, J.; Landreth, G.E.; Brosseron, F.; Feinstein, D.L.; Jacobs, A.H.; Wyss-Coray, T.; Vitorica, J.; Ransohoff, R.M.; et al. Neuroinflammation in Alzheimer's disease. *Lancet Neurol* **2015**, *14*, 388-405, doi:10.1016/S1474-4422(15)70016-5.
73. Zenaro, E.; Pietronigro, E.; Della Bianca, V.; Piacentino, G.; Marongiu, L.; Budui, S.; Turano, E.; Rossi, B.; Angiari, S.; Dusi, S.; et al. Neutrophils promote Alzheimer's disease-like pathology and cognitive decline via LFA-1 integrin. *Nature medicine* **2015**, *21*, 880-886, doi:10.1038/nm.3913.

74. Song, Z.; Bhattacharya, S.; Clemens, R.A.; Dinauer, M.C. Molecular regulation of neutrophil swarming in health and disease: Lessons from the phagocyte oxidase. *iScience* **2023**, *26*, 108034, doi:10.1016/j.isci.2023.108034.
75. Lammermann, T. In the eye of the neutrophil swarm-navigation signals that bring neutrophils together in inflamed and infected tissues. *J Leukoc Biol* **2016**, *100*, 55-63, doi:10.1189/jlb.1MR0915-403.
76. Nitta, T.; Hata, M.; Gotoh, S.; Seo, Y.; Sasaki, H.; Hashimoto, N.; Furuse, M.; Tsukita, S. Size-selective loosening of the blood-brain barrier in claudin-5-deficient mice. *J Cell Biol* **2003**, *161*, 653-660, doi:10.1083/jcb.200302070.
77. Shadfar, S.; Hwang, C.J.; Lim, M.S.; Choi, D.Y.; Hong, J.T. Involvement of inflammation in Alzheimer's disease pathogenesis and therapeutic potential of anti-inflammatory agents. *Arch Pharm Res* **2015**, *38*, 2106-2119, doi:10.1007/s12272-015-0648-x.
78. Iqbal, K.; Grundke-Iqbal, I. Alzheimer's disease, a multifactorial disorder seeking multitherapies. *Alzheimers Dement* **2010**, *6*, 420-424, doi:10.1016/j.jalz.2010.04.006.
79. Carreiras, M.C.; Mendes, E.; Perry, M.J.; Francisco, A.P.; Marco-Contelles, J. The multifactorial nature of Alzheimer's disease for developing potential therapeutics. *Curr Top Med Chem* **2013**, *13*, 1745-1770, doi:10.2174/15680266113139990135.
80. Erdo, F.; Bors, L.A.; Farkas, D.; Bajza, A.; Gizurarson, S. Evaluation of intranasal delivery route of drug administration for brain targeting. *Brain Res Bull* **2018**, *143*, 155-170, doi:10.1016/j.brainresbull.2018.10.009.
81. Lochhead, J.J.; Thorne, R.G. Intranasal delivery of biologics to the central nervous system. *Adv Drug Deliv Rev* **2012**, *64*, 614-628, doi:10.1016/j.addr.2011.11.002.
82. Chauhan, M.B.; Chauhan, N.B. Brain Uptake of Neurotherapeutics after Intranasal versus Intraperitoneal Delivery in Mice. *J Neurol Neurosurg* **2015**, *2*.
83. Louneva, N.; Cohen, J.W.; Han, L.Y.; Talbot, K.; Wilson, R.S.; Bennett, D.A.; Trojanowski, J.Q.; Arnold, S.E. Caspase-3 is enriched in postsynaptic densities and increased in Alzheimer's disease. *Am J Pathol* **2008**, *173*, 1488-1495, doi:10.2353/ajpath.2008.080434.
84. Cunningham, C.; Wilcockson, D.C.; Campion, S.; Lunnon, K.; Perry, V.H. Central and systemic endotoxin challenges exacerbate the local inflammatory response and increase neuronal death during chronic neurodegeneration. *J Neurosci* **2005**, *25*, 9275-9284, doi:10.1523/JNEUROSCI.2614-05.2005.
85. Sil, S.; Ghosh, T. Role of cox-2 mediated neuroinflammation on the neurodegeneration and cognitive impairments in colchicine induced rat model of Alzheimer's Disease. *J Neuroimmunol* **2016**, *291*, 115-124, doi:10.1016/j.jneuroim.2015.12.003.
86. Singhal, G.; Jaehne, E.J.; Corrigan, F.; Toben, C.; Baune, B.T. Inflammasomes in neuroinflammation and changes in brain function: a focused review. *Front Neurosci* **2014**, *8*, 315, doi:10.3389/fnins.2014.00315.
87. Mackenzie, I.R.; Hao, C.; Munoz, D.G. Role of microglia in senile plaque formation. *Neurobiology of aging* **1995**, *16*, 797-804, doi:10.1016/0197-4580(95)00092-s.
88. Stalder, M.; Phinney, A.; Probst, A.; Sommer, B.; Staufenbiel, M.; Jucker, M. Association of microglia with amyloid plaques in brains of APP23 transgenic mice. *Am J Pathol* **1999**, *154*, 1673-1684, doi:10.1016/S0002-9440(10)65423-5.
89. Yan, P.; Bero, A.W.; Cirrito, J.R.; Xiao, Q.; Hu, X.; Wang, Y.; Gonzales, E.; Holtzman, D.M.; Lee, J.M. Characterizing the appearance and growth of amyloid plaques in APP/PS1 mice. *J Neurosci* **2009**, *29*, 10706-10714, doi:10.1523/JNEUROSCI.2637-09.2009.
90. Bolmont, T.; Haiss, F.; Eicke, D.; Radde, R.; Mathis, C.A.; Klunk, W.E.; Kohsaka, S.; Jucker, M.; Calhoun, M.E. Dynamics of the microglial/amyloid interaction indicate a role in plaque maintenance. *J Neurosci* **2008**, *28*, 4283-4292, doi:10.1523/JNEUROSCI.4814-07.2008.
91. Mandrekar-Colucci, S.; Landreth, G.E. Microglia and inflammation in Alzheimer's disease. *CNS Neurol Disord Drug Targets* **2010**, *9*, 156-167, doi:10.2174/187152710791012071.
92. Cai, Z.; Hussain, M.D.; Yan, L.J. Microglia, neuroinflammation, and beta-amyloid protein in Alzheimer's disease. *Int J Neurosci* **2014**, *124*, 307-321, doi:10.3109/00207454.2013.833510.
93. Shrivastava, P.; Vaibhav, K.; Tabassum, R.; Khan, A.; Ishrat, T.; Khan, M.M.; Ahmad, A.; Islam, F.; Safhi, M.M.; Islam, F. Anti-apoptotic and anti-inflammatory effect of Piperine on 6-OHDA induced Parkinson's rat model. *J Nutr Biochem* **2013**, *24*, 680-687, doi:10.1016/j.jnutbio.2012.03.018.
94. Franco-Bocanegra, D.K.; Gourari, Y.; McAuley, C.; Chatelet, D.S.; Johnston, D.A.; Nicoll, J.A.R.; Boche, D. Microglial morphology in Alzheimer's disease and after Abeta immunotherapy. *Scientific reports* **2021**, *11*, 15955, doi:10.1038/s41598-021-95535-0.
95. Poplimont, H.; Georgantzoglou, A.; Boulch, M.; Walker, H.A.; Coombs, C.; Papaleonidopoulou, F.; Sarris, M. Neutrophil Swarming in Damaged Tissue Is Orchestrated by Connexins and Cooperative Calcium Alarm Signals. *Curr Biol* **2020**, *30*, 2761-2776 e2767, doi:10.1016/j.cub.2020.05.030.
96. Rosales, C. Neutrophil: A Cell with Many Roles in Inflammation or Several Cell Types? *Front Physiol* **2018**, *9*, 113, doi:10.3389/fphys.2018.00113.
97. Kotredes, K.P.; Pandey, R.S.; Persohn, S.; Elderidge, K.; Burton, C.P.; Miner, E.W.; Haynes, K.A.; Santos, D.F.S.; Williams, S.P.; Heaton, N.; et al. Characterizing molecular and synaptic signatures in mouse models

of late-onset Alzheimer's disease independent of amyloid and tau pathology. *Alzheimers Dement* **2024**, *20*, 4126-4146, doi:10.1002/alz.13828.
98. Oblak, A.L.; Forner, S.; Territo, P.R.; Sasner, M.; Carter, G.W.; Howell, G.R.; Sukoff-Rizzo, S.J.; Logsdon, B.A.; Mangravite, L.M.; Mortazavi, A.; et al. Model organism development and evaluation for late-onset Alzheimer's disease: MODEL-AD. *Alzheimers Dement (N Y)* **2020**, *6*, e12110, doi:10.1002/trc2.12110.
99. Sukoff Rizzo, S.J.; Masters, A.; Onos, K.D.; Quinney, S.; Sasner, M.; Oblak, A.; Lamb, B.T.; Territo, P.R.; consortium, M.-A. Improving preclinical to clinical translation in Alzheimer's disease research. *Alzheimers Dement (N Y)* **2020**, *6*, e12038, doi:10.1002/trc2.12038.
100. Forner, S.; Kawauchi, S.; Balderrama-Gutierrez, G.; Kramar, E.A.; Matheos, D.P.; Phan, J.; Javonillo, D.I.; Tran, K.M.; Hingco, E.; da Cunha, C.; et al. Systematic phenotyping and characterization of the 5xFAD mouse model of Alzheimer's disease. *Sci Data* **2021**, *8*, 270, doi:10.1038/s41597-021-01054-y.
101. Chen, C.; Wei, J.; Ma, X.; Xia, B.; Shakir, N.; Zhang, J.K.; Zhang, L.; Cui, Y.; Ferguson, D.; Qiu, S.; et al. Disrupted Maturation of Prefrontal Layer 5 Neuronal Circuits in an Alzheimer's Mouse Model of Amyloid Deposition. *Neurosci Bull* **2023**, *39*, 881-892, doi:10.1007/s12264-022-00951-5.